# Konkoly Observatory's research achievements in 2016

Annual research evaluation meeting, 23 February 2017

# Agenda

- Publications in 2016
- Highlights of the results
- Individual research evaluation
- Research group reports

# Overview of the institute's publications

# Overview of the publications in 2016

- **104** papers in journals with ISI impact factors, cumulative i.f. **589.4 (5.67/paper)**
- **248** scientific publications
- First-authored refereed papers: **39**
- Number of staff: 53 (1 member of MTA, 5 emeriti, 3 D.Sc., 25 PhD, 19 without PhD)

# 2016 publications

- 31 A&A
- 6 AJ
- 21 ApJ
- 2 ApJL
- 4 ApJS
- 1 AstroBio.
- 1 CeMDA
- 1 Climate Dyn.
- 1 Exp. Astron.
- 1 Geochim.C.Acta
- 1 IJMPE
- 17 MNRAS
- 1 Nature
- 1 New. Astron.
- 3 OLEB
- 1 Planet. Sp. Sci.
- 1 PASP
- 3 Phys.Rev.C
- 1 PNAS
- 1 Science
- 1 Sci.China Phys.M.Ast.
- 4 Solar Phys.
- 1 Sp.Sci.Rev.

**71% in "three" journals**

# Refereed papers: types and facilities

- **Theory/review:** 28
- **Ground based data**
  - Piszkéstető 6
  - Debrecen 4
  - HATNet 1
  - Fly’s Eye 1
  - ESO/ ALMA(APEX) 2
  - other /collections 17
- **Space observatories**
  - Herschel 6
  - Kepler/K2 7
  - Solar probes 4
  - CoRoT, MOST 4
  - HST 1
  - Gaia 3
  - Rosetta 9
  - other 8
- **Laboratory** 5

# Konkoly ISI papers 2006-2016

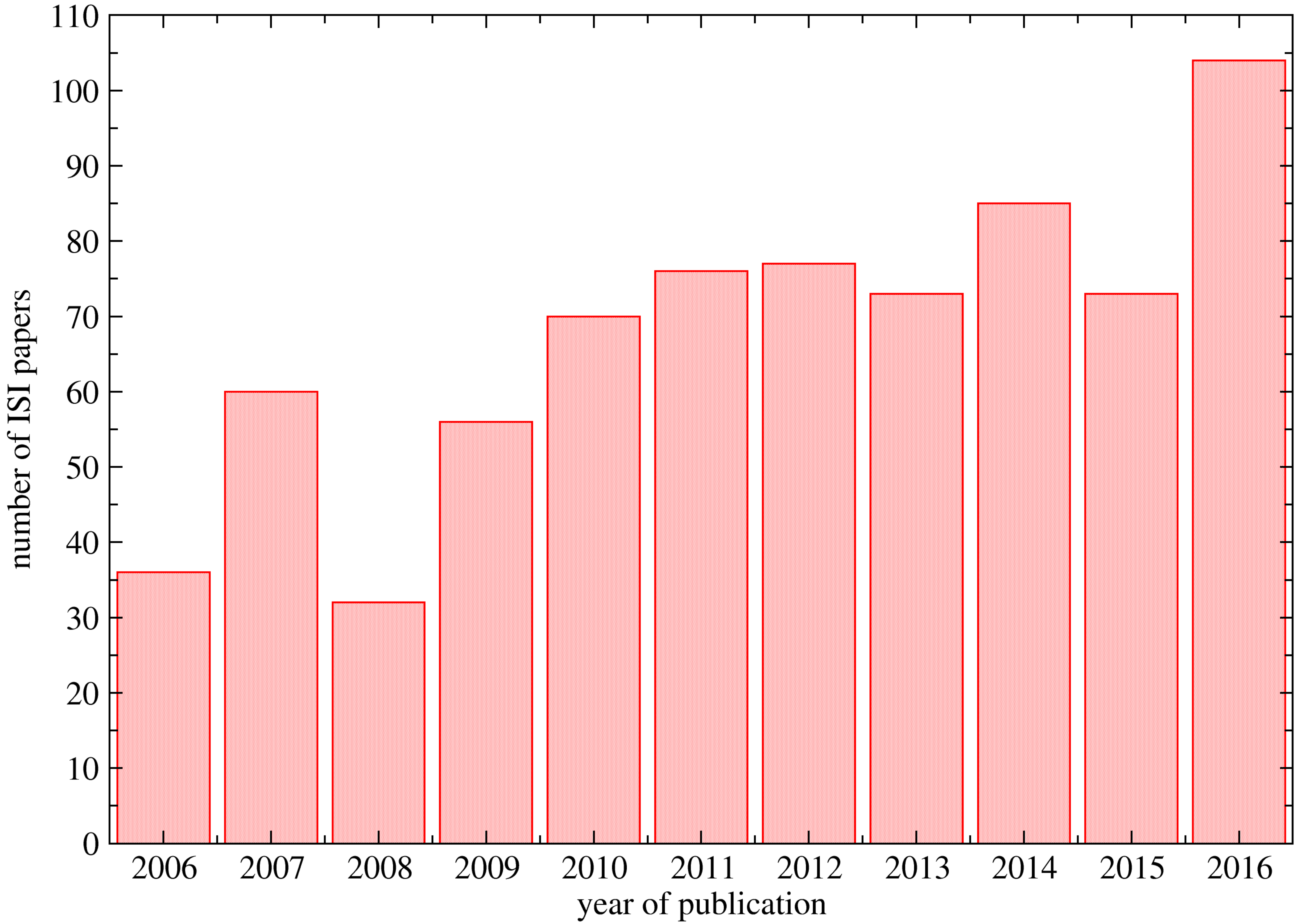

# Konkoly ISI papers per FTE 2006-2016

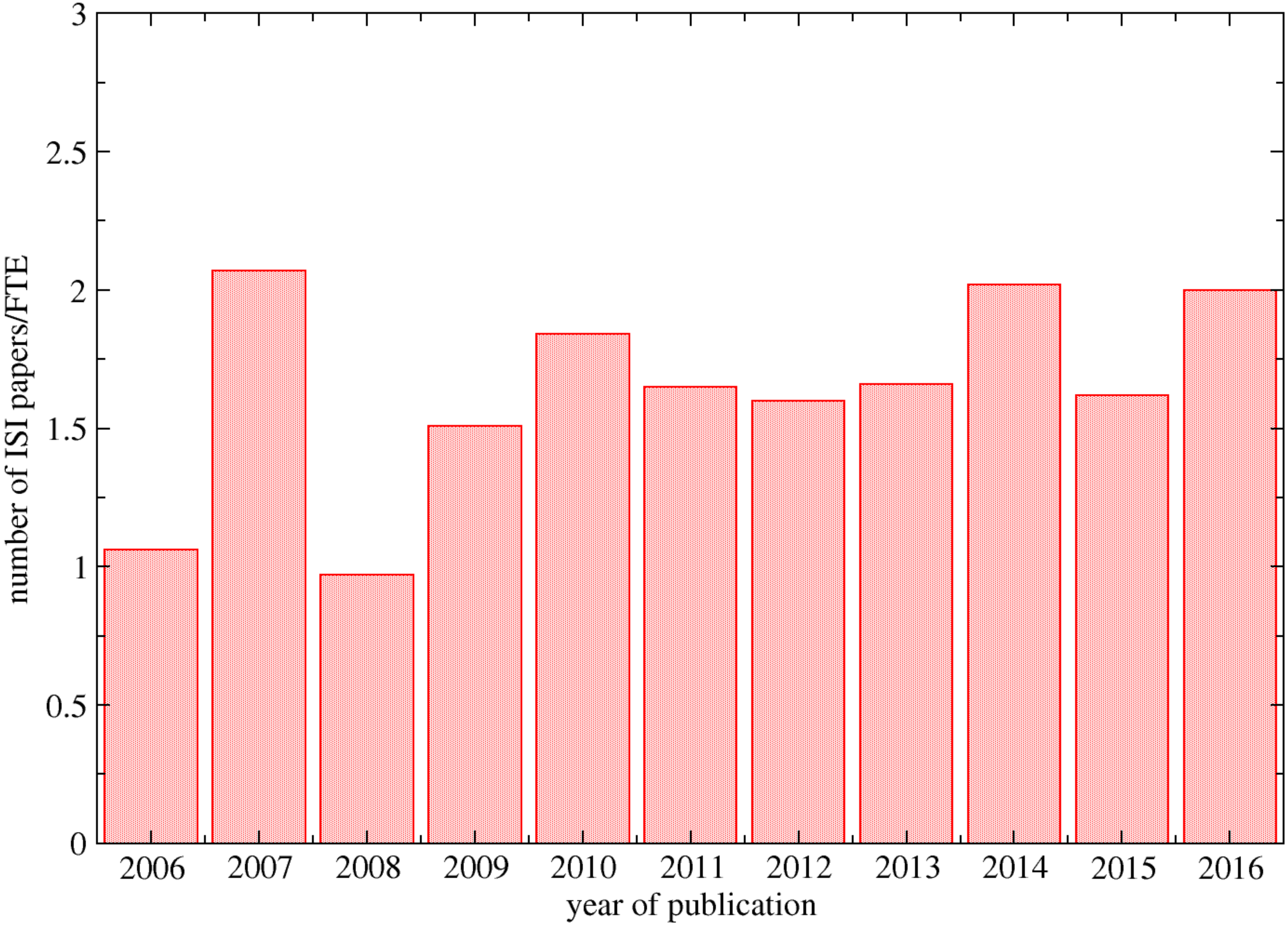

# Konkoly cumulative impact factor 2006-2016

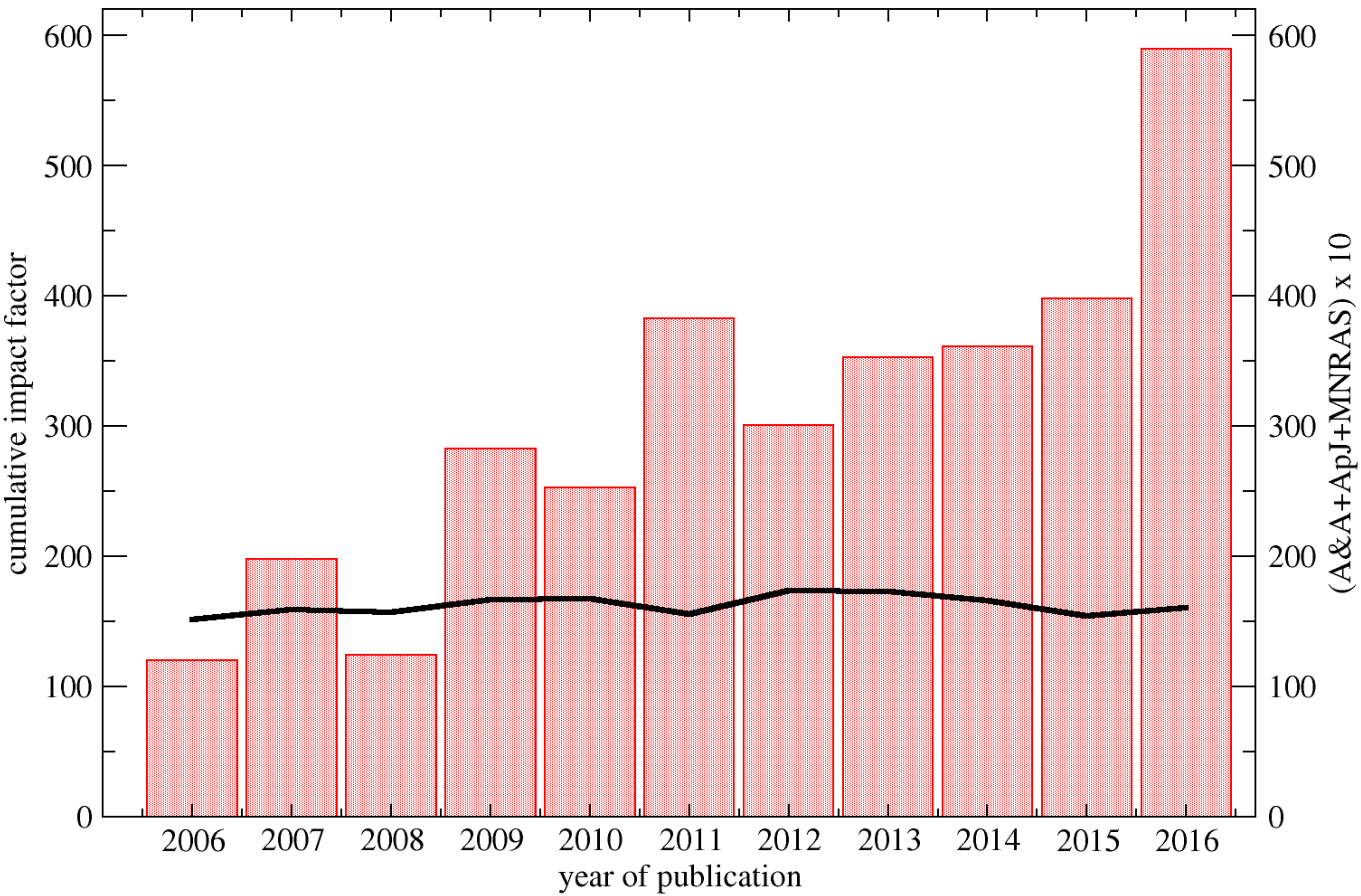

# Konkoly cumulative impact factor per FTE 2006-2016

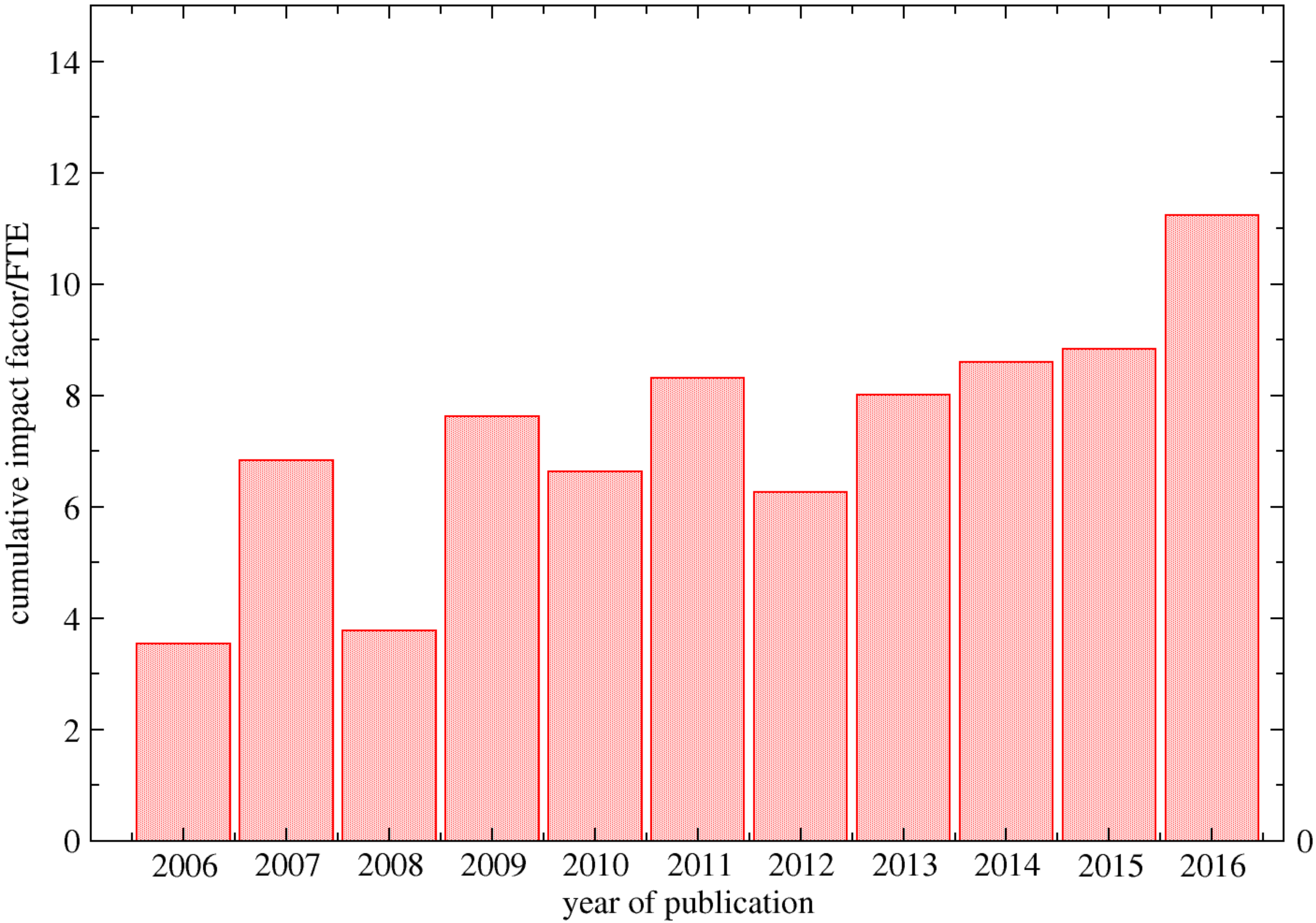

# Konkoly independent citations 2006-2016

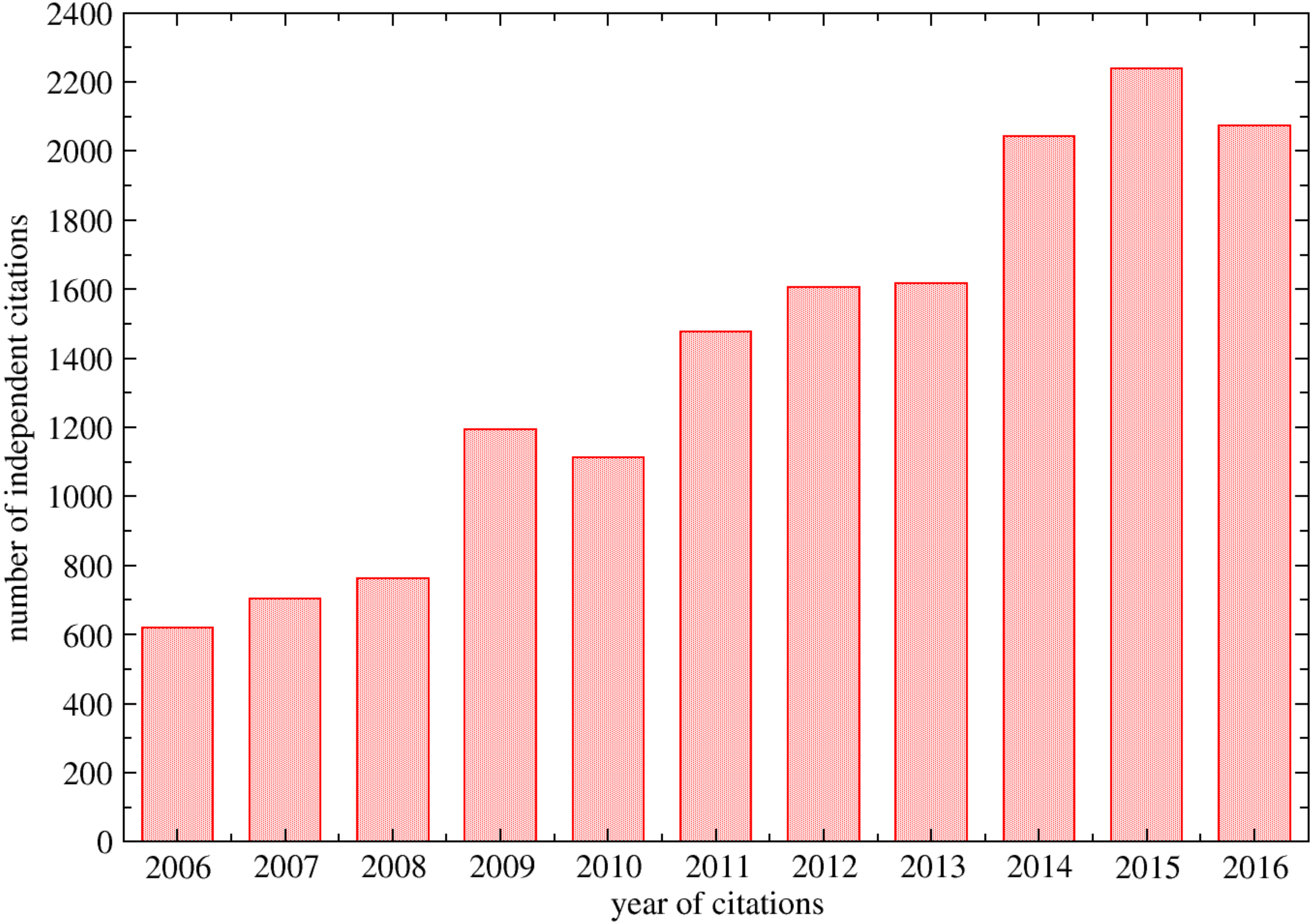

# Konkoly ISI publications 2016

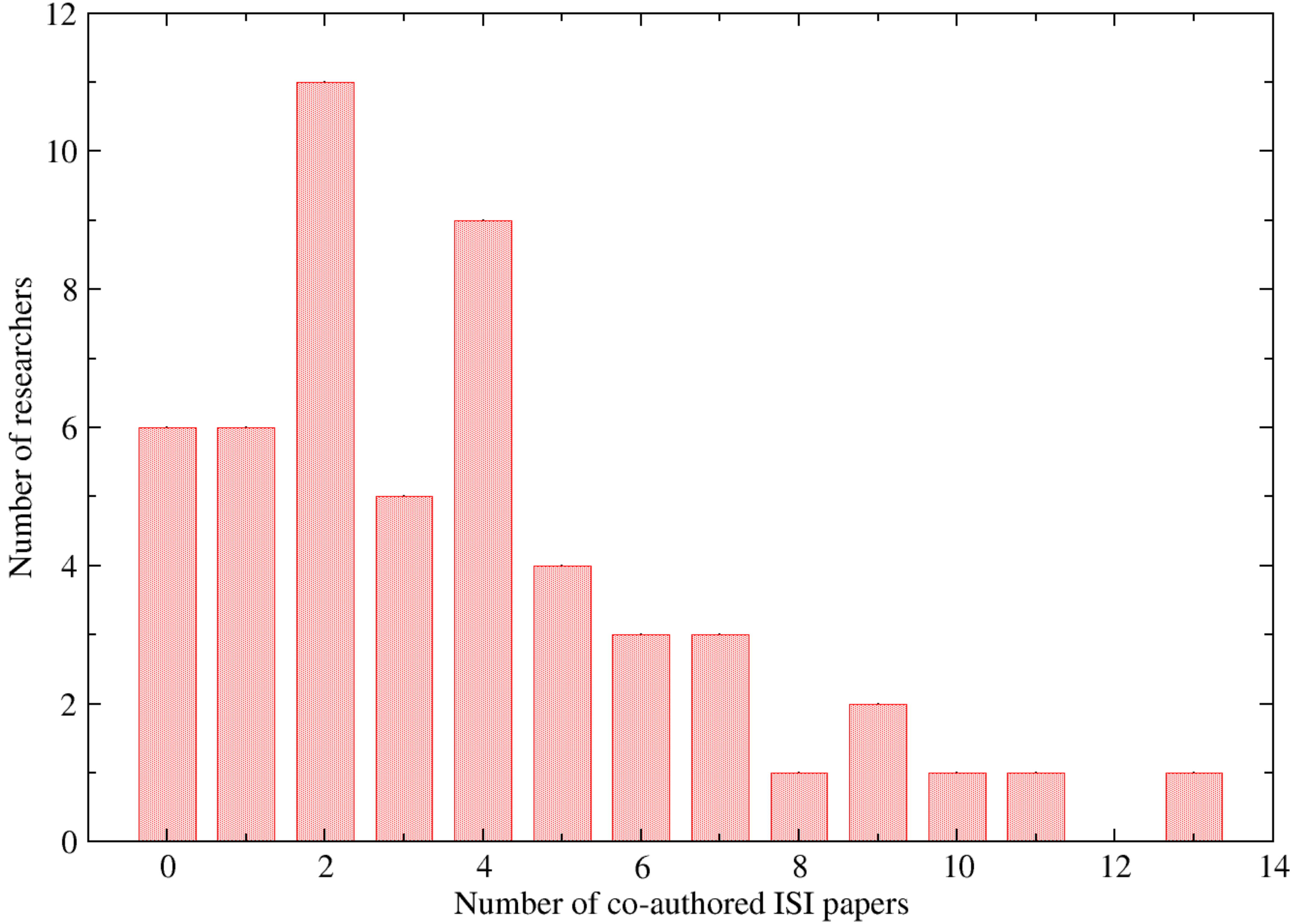


13 Pignatari M.

11 Pál A.

10 Tóth I.

9 Moór A.
Vida K.

8 Molnár L.

7 Kiss Cs.
Kiss L.
Sárneczky K.

6 Kereszturi Á.
Kóspál Á.
Lugaro M.

5 Oláh K.
Skarka M.
Sódor Á.
Szabó R.

# Konkoly Observatory – author numbers

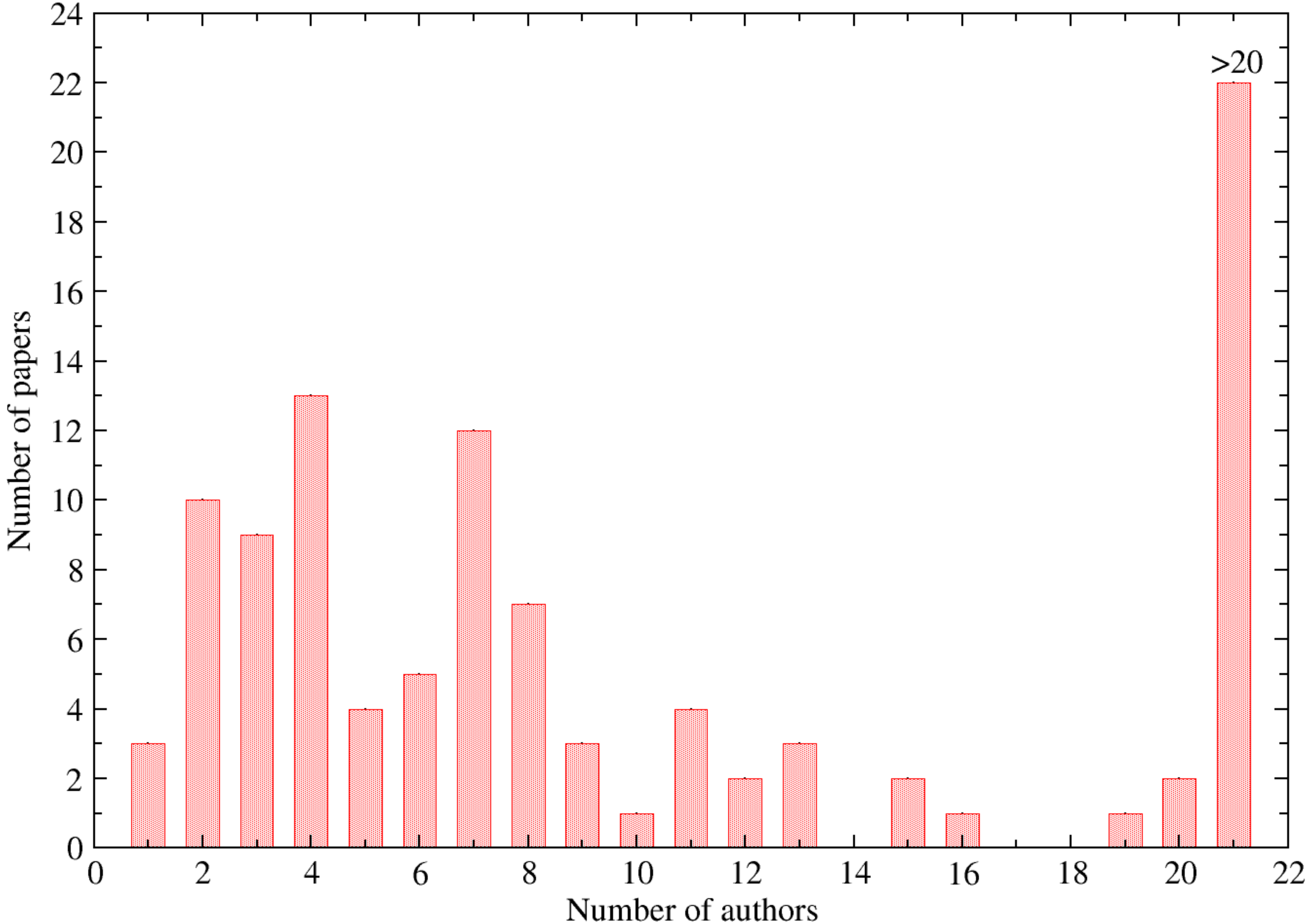

# 2016/2017: the beginning of a new era supported by large grants

- GINOP Strategic R+D (L. Kiss, Cosmic effects and risks, 2.3 MEUR, Oct. 3, 2016 + 4 yrs)

- GINOP Strategic R+D (J. Vinkó, Transient Astrophysical Objects, 1.3 MEUR, Jan. 2, 2017 + 4 yrs)

- ERC Starting Grant (Á. Kóspál, Structured Accretion Disks, 1.3 MEUR, July 1, 2017 + 5 yrs)

- ERC Consolidator Grant (M. Lugaro, Radioactivities from stars to Solar System
  1.7 MEUR, Sept. 1, 2017 + 5 yrs)

**Total grant income in 2016 is approximately 9 MEUR for the period 2017-2022 (cf. annual budget of Konkoly: ~1 MEUR)**

# A quick SWOT-analysis

- **Strength**: excellent team of internationally recognized researchers
- **Weakness**: one sided scientific profile (predominantly stellar physics)
- **Opportunity**: new EU/ESA/local funding opportunities
- **Threat**: turbulent legal and economic situation, keeping the best researchers

# Highlights

# Origin of the *p*-process radionuclides $^{92}$Nb and $^{146}$Sm in the early solar system and inferences on the birth of the Sun

**Maria Lugaro[a,b,1], Marco Pignatari[a,c], Ulrich Ott[d,e], Kai Zuber[f], Claudia Travaglio[c,g], György Gyürky[h], and Zsolt Fülöp[h]**

[a]Konkoly Observatory, Research Centre for Astronomy and Earth Sciences, Hungarian Academy of Sciences, H-1121 Budapest, Hungary; [b]Monash Centre for Astrophysics, Monash University, Clayton, VIC 3800, Australia; [c]NuGrid Collaboration; [d]Faculty of Natural Science, University of West Hungary, H-9700 Szombathely, Hungary; [e]Max Planck Institute for Chemistry, D-55128 Mainz, Germany; [f]Institut für Kern- und Teilchenphysik, Technische Universität Dresden, D-01069 Dresden, Germany; [g]Osservatorio di Torino, I-10025 Pino Torinese, Italy; and [h]Atomki Institute for Nuclear Research, Hungarian Academy of Sciences, H-4001 Debrecen, Hungary

Edited by Neta A. Bahcall, Princeton University, Princeton, NJ, and approved December 7, 2015 (received for review September 29, 2015)

**The abundances of $^{92}$Nb and $^{146}$Sm in the early solar system are determined from meteoritic analysis, and their stellar production is attributed to the *p* process. We investigate if their origin from thermonuclear supernovae deriving from the explosion of white dwarfs with mass above the Chandrasekhar limit is in agreement with the abundance of $^{53}$Mn, another radionuclide present in the early solar system and produced in the same events. A consistent solution for $^{92}$Nb and $^{53}$Mn cannot be found within the current uncertainties and requires the $^{92}$Nb/$^{92}$Mo ratio in the early solar system to be at least 50% lower than the current nominal value, which is outside its present error bars. A different solution is to invoke another production site for $^{92}$Nb, which we find in the α-rich freezeout during core-collapse supernovae from massive stars. Whichever scenario we consider, we find that a relatively long time interval of at least ∼10 My must have elapsed from when the star-forming region where the Sun was born was isolated from the interstellar medium and the birth of the Sun. This is in agreement with results obtained from radionuclides heavier than iron produced by neutron captures and lends further support to the idea that the Sun was born in a massive star-forming region together with many thousands of stellar siblings.**

short-lived radionuclides | solar system formation | supernovae

Here, we turn to the investigation of the origin of the other two radionuclides heavier than Fe whose abundances are well known in the ESS: $^{92}$Nb and $^{146}$Sm. These nuclei are proton-rich, relative to the stable nuclei of Nb and Sm, which means that they cannot be produced by neutron captures like the vast majority of the nuclei heavier than Fe. Instead, their nucleosynthetic origin has been traditionally ascribed to some flavor of the so-called *p* process (4, 5), for example, the disintegration of heavier nuclei (γ-process). Unfortunately, the possible astrophysical sites of origin of *p*-process nuclei in the universe are not well-constrained.

Core-collapse supernova (CCSN) explosions (6) deriving from the final collapse of massive stars have been considered as a possible site for the γ-process, specifically, the O–Ne-rich zones of the CCSN ejecta (7). However, models never managed to reproduce the complete *p*-process pattern observed in the bulk of the solar system material (8–10). For instance, CCSN models cannot reproduce the relatively large abundances of $^{92,94}$Mo and $^{96,98}$Ru. Taking into account nuclear uncertainties has not solved the problem (11, 12), except for a possible increase of the $^{12}$C+$^{12}$C fusion reaction rate (13, 14). Another process in core-collapse supernovae (CCSNe) that can produce the light *p*-process nuclei

# LETTER

doi:10.1038/nature17444

# No Sun-like dynamo on the active star ζ Andromedae from starspot asymmetry

R. M. Roettenbacher[1], J. D. Monnier[1], H. Korhonen[2,3], A. N. Aarnio[1], F. Baron[1,4], X. Che[1], R. O. Harmon[5], Zs. Kővári[6], S. Kraus[1,7], G. H. Schaefer[8], G. Torres[9], M. Zhao[1,10], T. A. ten Brummelaar[8], J. Sturmann[8] & L. Sturmann[8]

**Sunspots are cool areas caused by strong surface magnetic fields that inhibit convection[1,2]. Moreover, strong magnetic fields can alter the average atmospheric structure[3], degrading our ability to measure stellar masses and ages. Stars that are more active than the Sun have more and stronger dark spots than does the Sun, including on the rotational pole[4]. Doppler imaging, which has so far produced the most detailed images of surface structures on other stars, cannot always distinguish the hemisphere in which the starspots are located, especially in the equatorial region and if the data quality is not optimal[5]. This leads to problems in investigating the north–south distribution of starspot active latitudes (those latitudes with more starspot activity); this distribution is a crucial constraint of dynamo theory. Polar spots, whose existence is inferred from Doppler tomography, could plausibly be observational artefacts[6]. Here we report imaging of the old, magnetically active star ζ Andromedae using long-baseline infrared interferometry. In our data, a dark polar spot is seen in each of two observation epochs, whereas lower-latitude spot structures in both hemispheres do not persist between observations, revealing global starspot asymmetries. The north–south symmetry of active latitudes observed on the Sun[7] is absent on ζ And, which hosts global spot patterns that cannot be produced by solar-type dynamos[8].**

The surface temperature maps for ζ And show peaks of 4,530 K and 4,550 K and minimum values of 3,540 K and 3,660 K in 2011 and 2013, respectively. The ∼900-K range of temperatures we see across the surface is slightly larger than the ∼700-K range found from recent Doppler imaging work (from the Fe I $\lambda = 6,430$ Å line). A strong dark polar spot is present in both of our imaging epochs, also consistent with recent Doppler imaging studies[7,13,14]. In contrast to this persistent feature, many other large dark regions change completely between 2011 and 2013 with no apparent overall symmetry or pattern. These features and their locations can only unambiguously be imaged by interferometry, since Doppler and light-curve inversion imaging techniques experience latitude degeneracies (see Methods section for more details). We now discuss the starspot implications on the dynamical large-scale magnetic field of ζ And.

The extended network of cool regions stretching across the star suggest that strong magnetic fields can suppress convection on global scales, rather than just local concentrations forming spot structures. The extent to which starspots can cover the surface of a star is at present unknown and of interest in understanding how activity saturates on rapidly rotating, convective stars[15]. The observations in hand lend support to studies that have suggested magnetic activity can be so widespread as to alter the apparent fundamental parameters of a star[16,17]. For example, a larger region of suppressed convection gives

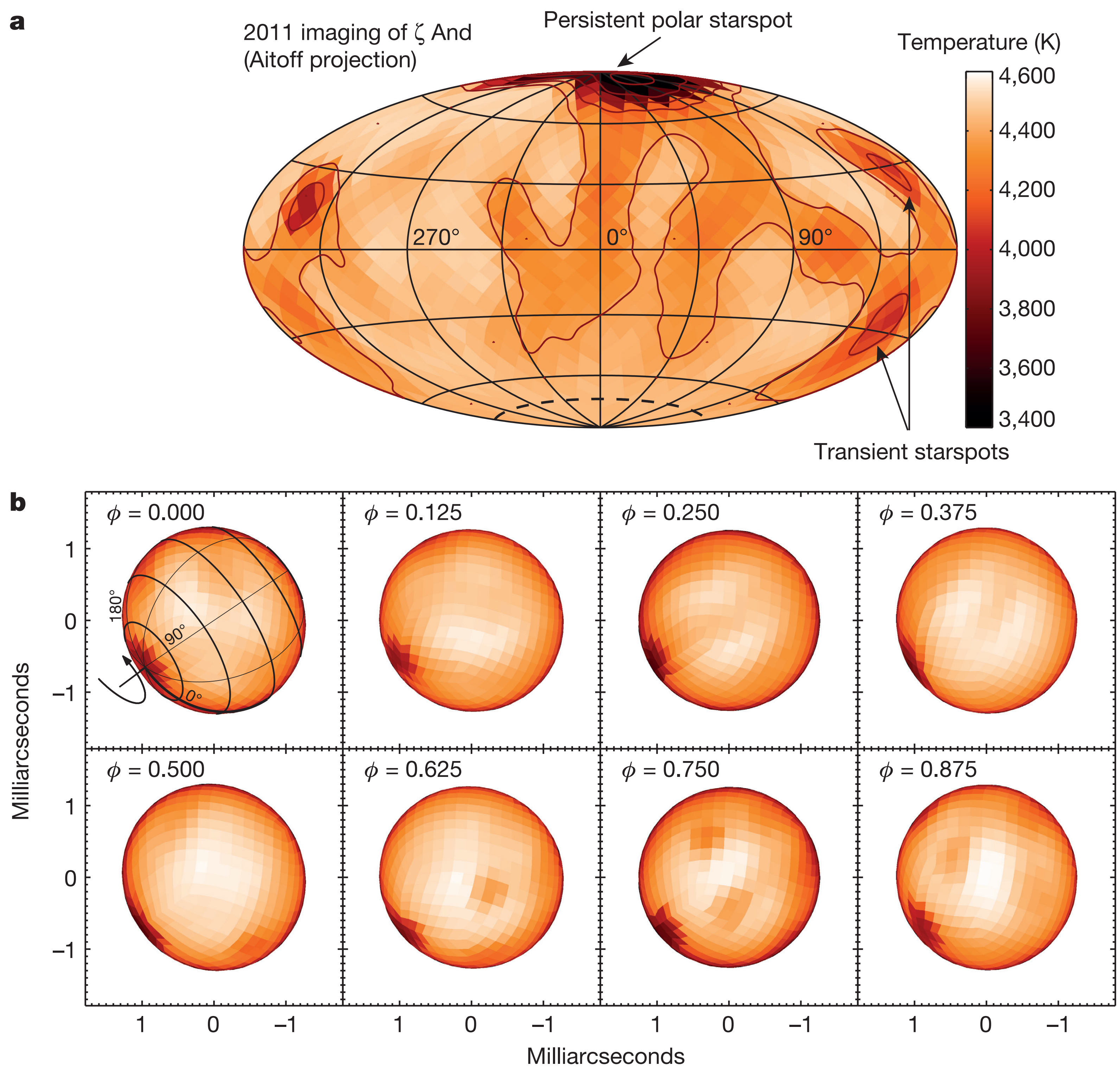


**Figure 1 | Surface image of ζ And from July 2011 with eleven nights of data using SURFING. a,** The temperature of ζ And is presented in an Aitoff projection. The contours represent every 200 K from 3,400 K to 4,600 K. The dashed line at the bottom pole indicates the latitudes below, which are hidden owing to the inclination. Arrows point to example transient starspots. **b,** The surface reflects how the star is observed on the sky with *H*-band intensities (mean $H = 1.64$). The phase $\phi = 0.000$ plot shows longitude 0° at the bottom right of the star with 90° across the middle. The phases assume circular orbit radial velocity conventions. The images are oriented with north up and east to the left.

COMETARY SCIENCE

# Rosetta's comet 67P/Churyumov-Gerasimenko sheds its dusty mantle to reveal its icy nature

S. Fornasier,[1*] S. Mottola,[2] H. U. Keller,[2,3] M. A. Barucci,[1] B. Davidsson,[4] C. Feller,[1] J. D. P. Deshapriya,[1] H. Sierks,[5] C. Barbieri,[6] P. L. Lamy,[7] R. Rodrigo,[8,9] D. Koschny,[10] H. Rickman,[11,12] M. A'Hearn,[13] J. Agarwal,[5] J.-L. Bertaux,[14] I. Bertini,[6] S. Besse,[15] G. Cremonese,[16] V. Da Deppo,[17] S. Debei,[18] M. De Cecco,[19] J. Deller,[5] M. R. El-Maarry,[20] M. Fulle,[21] O. Groussin,[22] P. J. Gutierrez,[8] C. Güttler,[5] M. Hofmann,[5] S. F. Hviid,[2] W.-H. Ip,[23,24] L. Jorda,[22] J. Knollenberg,[2] G. Kovacs,[5,25] R. Kramm,[5] E. Kührt,[2] M. Küppers,[15] M. L. Lara,[8] M. Lazzarin,[6] J. J. Lopez Moreno,[8] F. Marzari,[6] M. Massironi,[26,27] G. Naletto,[28,27,17] N. Oklay,[5] M. Pajola,[29,27] A. Pommerol,[20] F. Preusker,[2] F. Scholten,[2] X. Shi,[5] N. Thomas,[20] I. Toth,[30] C. Tubiana,[5] J.-B. Vincent[5]

The Rosetta spacecraft has investigated comet 67P/Churyumov-Gerasimenko from large heliocentric distances to its perihelion passage and beyond. We trace the seasonal and diurnal evolution of the colors of the 67P nucleus, finding changes driven by sublimation and recondensation of water ice. The whole nucleus became relatively bluer near perihelion, as increasing activity removed the surface dust, implying that water ice is widespread underneath the surface. We identified large (1500 square meters) ice-rich patches appearing and then vanishing in about 10 days, indicating small-scale heterogeneities on the nucleus. Thin frosts sublimating in a few minutes are observed close to receding shadows, and rapid variations in color are seen on extended areas close to the terminator. These cyclic processes are widespread and lead to continuously, slightly varying surface properties.

All cometary nuclei observed to date have appeared to be dark, with only a limited amount of water ice detected in small patches (*1*, *2*), although water is the dominant volatile observed in their coma.

The Rosetta spacecraft has been orbiting comet 67P/Churyumov-Gerasimenko since August 2014, providing the opportunity to continuously investigate its nucleus. The comet has a distinct bilobate shape and a complex morphology (*3*–*5*), with a

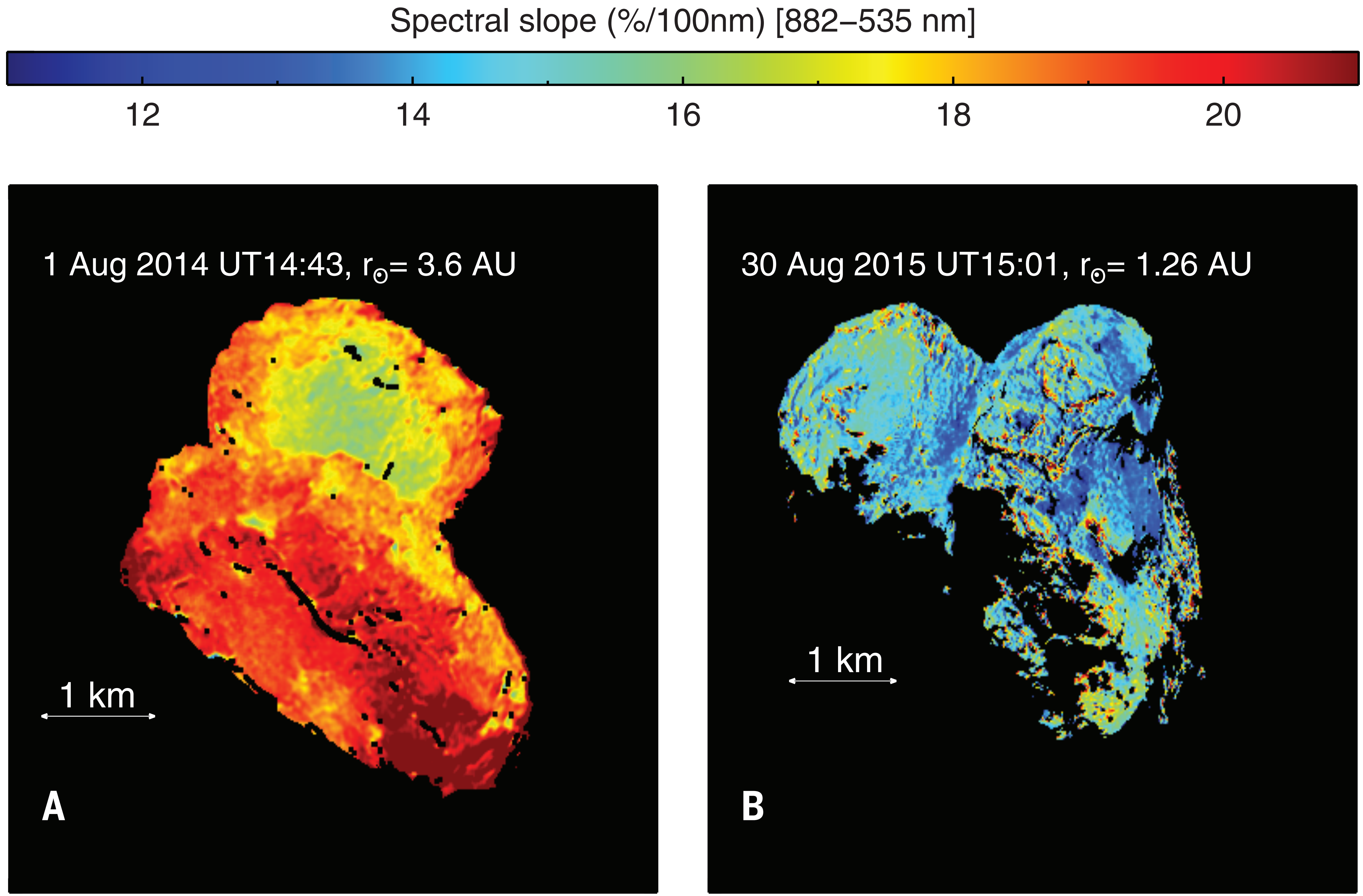


**Fig. 1. Spectral slope evolution with heliocentric distance.** The August 2014 image was corrected for the phase reddening from 10° to 70° using the coefficients published in (*15*) to match the viewing geometry on the right. See fig. S4 for the morphological regions context.

The Astrophysical Journal, 818:127 (8pp), 2016 February 20 doi:10.3847/0004-637X/818/2/127


# ACTIVE LONGITUDE AND SOLAR FLARE OCCURRENCES

N. Gyenge[1,2], A. Ludmány[1], and T. Baranyi[1]
[1] Debrecen Heliophysical Observatory (DHO), Konkoly Observatory, Research Centre for Astronomy and Earth Sciences, Hungarian Academy of Sciences Debrecen, P.O.Box 30, H-4010, Hungary; gyenge.norbert@csfk.mta.hu
[2] Solar Physics and Space Plasmas Research Centre (SP2RC), School of Mathematics and Statistics, University of Sheffield, Hounsfield Road, Hicks Building, Sheffield S3 7RH, UK
*Received 2015 July 29; accepted 2015 December 23; published 2016 February 16*

## ABSTRACT

The aim of the present work is to specify the spatio-temporal characteristics of flare activity observed by the *Reuven Ramaty High Energy Solar Spectroscopic Imager* (*RHESSI*) and the *Geostationary Operational Environmental Satellite* (*GOES*) in connection with the behavior of the longitudinal domain of enhanced sunspot activity known as active longitude (AL). By using our method developed for this purpose, we identified the AL in every Carrington Rotation provided by the Debrecen Photoheliographic Data. The spatial probability of flare occurrence has been estimated depending on the longitudinal distance from AL in the northern and southern hemispheres separately. We have found that more than 60% of the *RHESSI* and *GOES* flares is located within $\pm 36^{\circ}$ from the AL. Hence, the most flare-productive active regions tend to be located in or close to the active longitudinal belt. This observed feature may allow for the prediction of the geo-effective position of the domain of enhanced flaring probability. Furthermore, we studied the temporal properties of flare occurrence near the AL and several significant fluctuations were found. More precisely, the results of the method are the following fluctuations: 0.8, 1.3, and 1.8 years. These temporal and spatial properties of the solar flare occurrence within the active longitudinal belts could provide us with an enhanced solar flare forecasting opportunity.

*Key words:* Sun: activity – Sun: flares – sunspots

A&A 592, A139 (2016)
DOI: 10.1051/0004-6361/201526672


Astronomy & Astrophysics

# Possibility for albedo estimation of exomoons: Why should we care about M dwarfs?

Vera Dobos[1], Ákos Kereszturi[1], András Pál[1], and László L. Kiss[1,2]

[1] Konkoly Thege Miklós Astronomical Institute, Research Centre for Astronomy and Earth Sciences, Hungarian Academy of Sciences, 1121 Konkoly Thege Miklós út 15-17, Budapest, Hungary
e-mail: dobos@konkoly.hu
[2] Sydney Institute for Astronomy, School of Physics A28, University of Sydney, NSW 2006, Australia

Received 4 June 2015 / Accepted 4 June 2016

## ABSTRACT

Occultation light curves of exomoons may give information on the exomoons' albedo and hence indicate the presence of ice cover on the surface. Icy moons might have subsurface oceans, and thus may potentially be habitable. The objective of our paper is to determine whether next generation telescopes will be capable of albedo estimations for icy exomoons using their occultation light curves. The success of the measurements depends on the depth of the moon's occultation in the light curve and on the sensitivity of the used instruments. We applied simple calculations for different stellar masses in the *V* and *J* photometric bands, and compared the flux drop caused by the moon's occultation and the estimated photon noise of next generation missions with $5\sigma$ confidence. We found that albedo estimation by this method is not feasible for moons of solar-like stars, but small M dwarfs are better candidates for such measurements. Our calculations in the *J* photometric band show that E-ELT MICADO's photon noise is just about 4 ppm greater than the flux difference caused by an icy satellite twice the Earth's radius in a circular orbit at the snowline of an 0.1 stellar mass star. However, considering only photon noise underestimates the real expected noise, because other noise sources, such as CCD read-out and dark signal become significant in the near-infrared measurements. Hence we conclude that occultation measurements with next generation missions are far too challenging, even in the case of large, icy moons at the snowline of small M dwarfs. We also discuss the role of the parameters that were neglected in the calculations, for example inclination, eccentricity, orbiting direction of the moon. We predict that the first albedo estimations of exomoons will probably be made for large icy moons around the snowline of M4 – M9 type main sequence stars.

**Key words.** planets and satellites: surfaces – methods: numerical – planets and satellites: detection – occultations

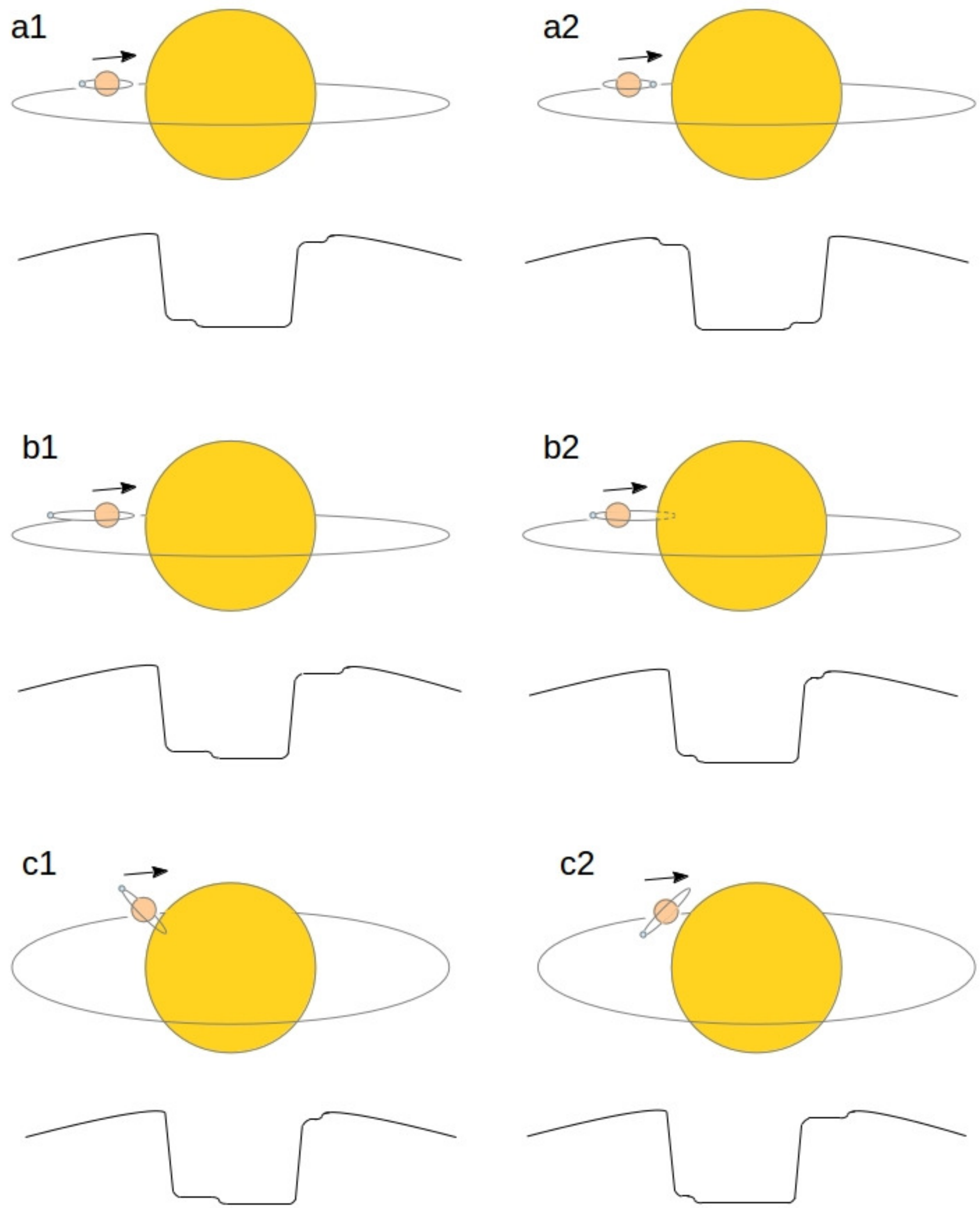
a1
a2
b1
b2
c1
c2

The Astrophysical Journal Supplement Series, 225:24 (54pp), 2016 August doi:10.3847/0067-0049/225/2/24


# NUGRID STELLAR DATA SET. I. STELLAR YIELDS FROM H TO BI FOR STARS WITH METALLICITIES $Z = 0.02$ and $Z = 0.01$

M. Pignatari[1,2,13], F. Herwig[3,4,13], R. Hirschi[5,6,13], M. Bennett[5,13], G. Rockefeller[7,13], C. Fryer[7,13], F. X. Timmes[4,8,13], C. Ritter[3,13], A. Heger[4,9,13], S. Jones[3,4,13], U. Battino[2,13], A. Dotter[10,13], R. Trappitsch[11,13], S. Diehl[7], U. Frischknecht[2], A. Hungerford[7,13], G. Magkotsios[4,13], C. Travaglio[12,13], and P. Young[8]

[1] E.A. Milne Centre for Astrophysics, Dept of Physics & Mathematics, University of Hull, HU6 7RX, United Kingdom
[2] Konkoly Observatory, Research Centre for Astronomy and Earth Sciences, Hungarian Academy of Sciences, Konkoly Thege Miklos ut 15-17, H-1121 Budapest, Hungary
[3] Department of Physics & Astronomy, University of Victoria, Victoria, BC, V8P5C2 Canada
[4] The Joint Institute for Nuclear Astrophysics, Notre Dame, IN 46556, USA
[5] Keele University, Keele, Staffordshire ST5 5BG, UK
[6] Institute for the Physics and Mathematics of the universe (WPI), University of Tokyo, 5-1-5 Kashiwanoha, Kashiwa 277-8583, Japan
[7] Computational Physics and Methods (CCS-2), LANL, Los Alamos, NM, 87545, USA
[8] Arizona State University (ASU), School of Earth and Space Exploration (SESE), P.O. Box 871404, Tempe, AZ, 85287-1404, USA
[9] Monash Centre for Astrophysics, School of Mathematical Sciences, Monash University, Vic 3800, Australia
[10] Research School of Astronomy and Astrophysics, Australian National University, Weston Creek, ACT 2611, Australia
[11] Department of the Geophysical Sciences and Chicago Center for Cosmochemistry, Chicago, IL 60637, USA
[12] Osservatorio Astronomico di Torino, Torino, Italy
*Received 2013 July 16; revised 2016 March 31; accepted 2016 April 4; published 2016 August 11*

## ABSTRACT

We provide a set of stellar evolution and nucleosynthesis calculations that applies established physics assumptions simultaneously to low- and intermediate-mass and massive star models. Our goal is to provide an internally consistent and comprehensive nuclear production and yield database for applications in areas such as presolar grain studies. Our non-rotating models assume convective boundary mixing (CBM) where it has been adopted before. We include 8 (12) initial masses for $Z = 0.01$ (0.02). Models are followed either until the end of the asymptotic giant branch phase or the end of Si burning, complemented by simple analytic core-collapse supernova (SN) models with two options for fallback and shock velocities. The explosions show which pre-SN yields will most strongly be effected by the explosive nucleosynthesis. We discuss how these two explosion parameters impact the light elements and the *s* and *p* process. For low- and intermediate-mass models, our stellar yields from H to Bi include the effect of CBM at the He-intershell boundaries and the stellar evolution feedback of the mixing process that produces the $^{13}$C pocket. All post-processing nucleosynthesis calculations use the same nuclear reaction rate network and nuclear physics input. We provide a discussion of the nuclear production across the entire mass range organized by element group. The entirety of our stellar nucleosynthesis profile and time evolution output are available electronically, and tools to explore the data on the NuGrid VOspace hosted by the Canadian Astronomical Data Centre are introduced.

*Key words:* nuclear reactions, nucleosynthesis, abundances – stars: abundances – stars: evolution – stars: interiors

*Supporting material:* machine-readable tables

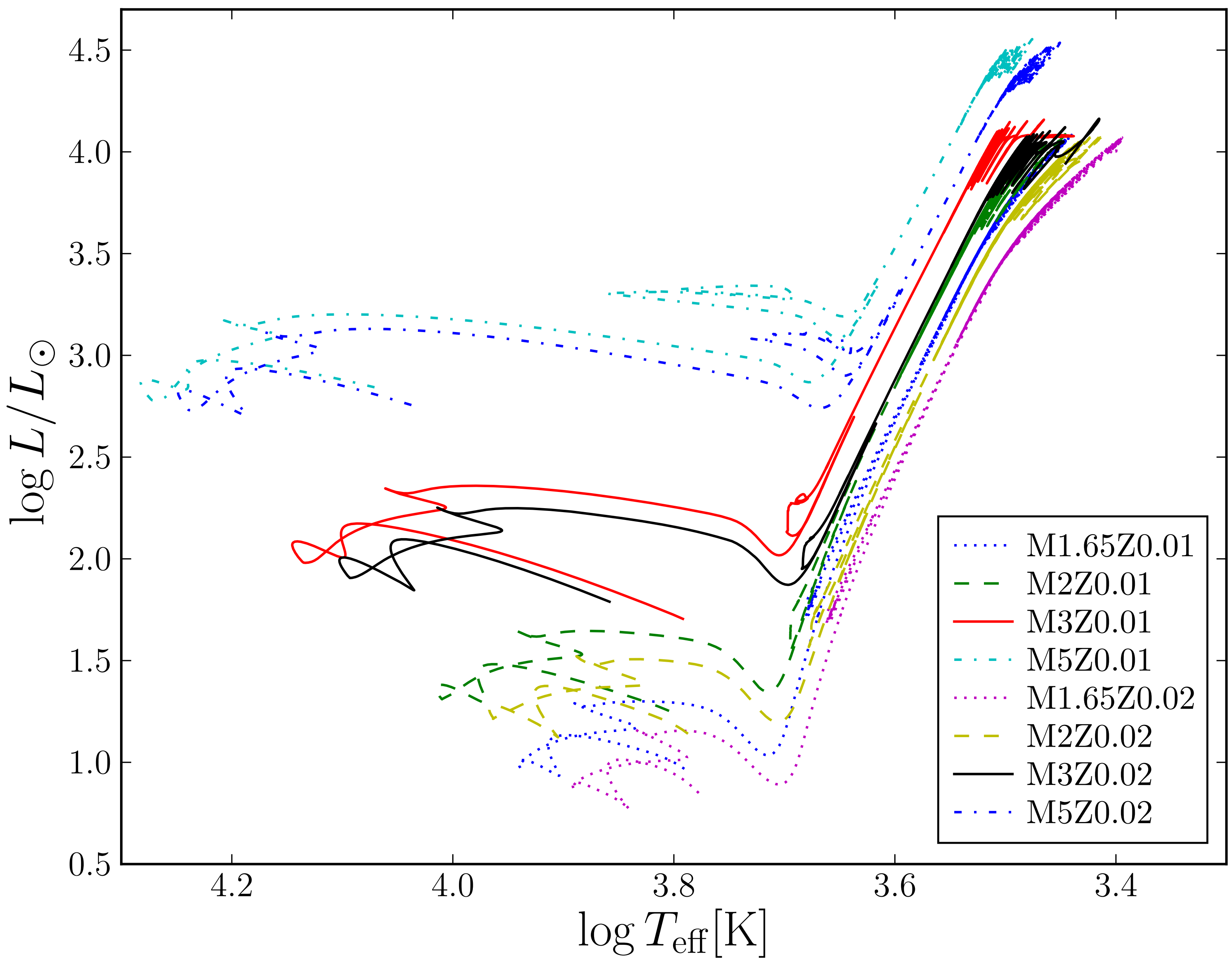


**Figure 1.** H–R diagram for low- and intermediate-mass models. Labels give the initial stellar mass followed by "S1" for Set 1.1 models ($Z = 0.01$) and "S2" for Set 1.2 models ($Z = 0.02$). Toward the end of the sequence, the tracks show wide loops, indicating an instability toward the end of the evolution that has been omitted from the plot for clarity (see the text for details).

A&A 596, A52 (2016)
DOI: 10.1051/0004-6361/201528061


Astronomy & Astrophysics

# Multiwavelength study of the low-luminosity outbursting young star HBC 722★

Á. Kóspál[1], P. Ábrahám[1], J. A. Acosta-Pulido[2,3], M. M. Dunham[4], D. García-Álvarez[2,3,5], M. R. Hogerheijde[6], M. Kun[1], A. Moór[1], A. Farkas[1], G. Hajdu[7,8], G. Hodosán[9], T. Kovács[1], L. Kriskovics[1], G. Marton[1], L. Molnár[1], A. Pál[1,10], K. Sárneczky[1], Á. Sódor[1], R. Szakáts[1], T. Szalai[11], E. Szegedi-Elek[1], A. Szing[12], I. Tóth[1], K. Vida[1], and J. Vinkó[1,11]

[1] Konkoly Observatory, Research Centre for Astronomy and Earth Sciences, Hungarian Academy of Sciences, PO Box 67, 1525 Budapest, Hungary
e-mail: kospal@konkoly.hu
[2] Instituto de Astrofísica de Canarias, Avenida Vía Láctea, 38205 La Laguna, Tenerife, Spain
[3] Departamento de Astrofísica, Universidad de La Laguna, 38205 La Laguna, Tenerife, Spain
[4] Harvard-Smithsonian Center for Astrophysics, 60 Garden Street, MS 78, Cambridge, MA 02138, USA
[5] Grantecan S. A., Centro de Astrofísica de La Palma, Cuesta de San José, 38712 Breña Baja, La Palma, Spain
[6] Leiden Observatory, Leiden University, Post Office Box 9513, 2300 RA Leiden, The Netherlands
[7] Instituto de Astrofísica, Facultad de Física, Pontificia Universidad Católica de Chile, Av. Vicuña Mackenna, 4860 Santiago, Chile
[8] Instituto Milenio de Astrofísica, Santiago, Chile
[9] University of St Andrews, School of Physics & Astronomy, St. Andrews, UK
[10] Department of Astronomy, Loránd Eötvös University, Pázmány Péter sétány 1/A, 1117 Budapest, Hungary
[11] Department of Optics and Quantum Electronics, University of Szeged, Dóm tér 9., 6720 Szeged, Hungary
[12] Baja Observatory, University of Szeged, 6500 Baja, KT. 766, Hungary

Received 30 December 2015 / Accepted 11 July 2016

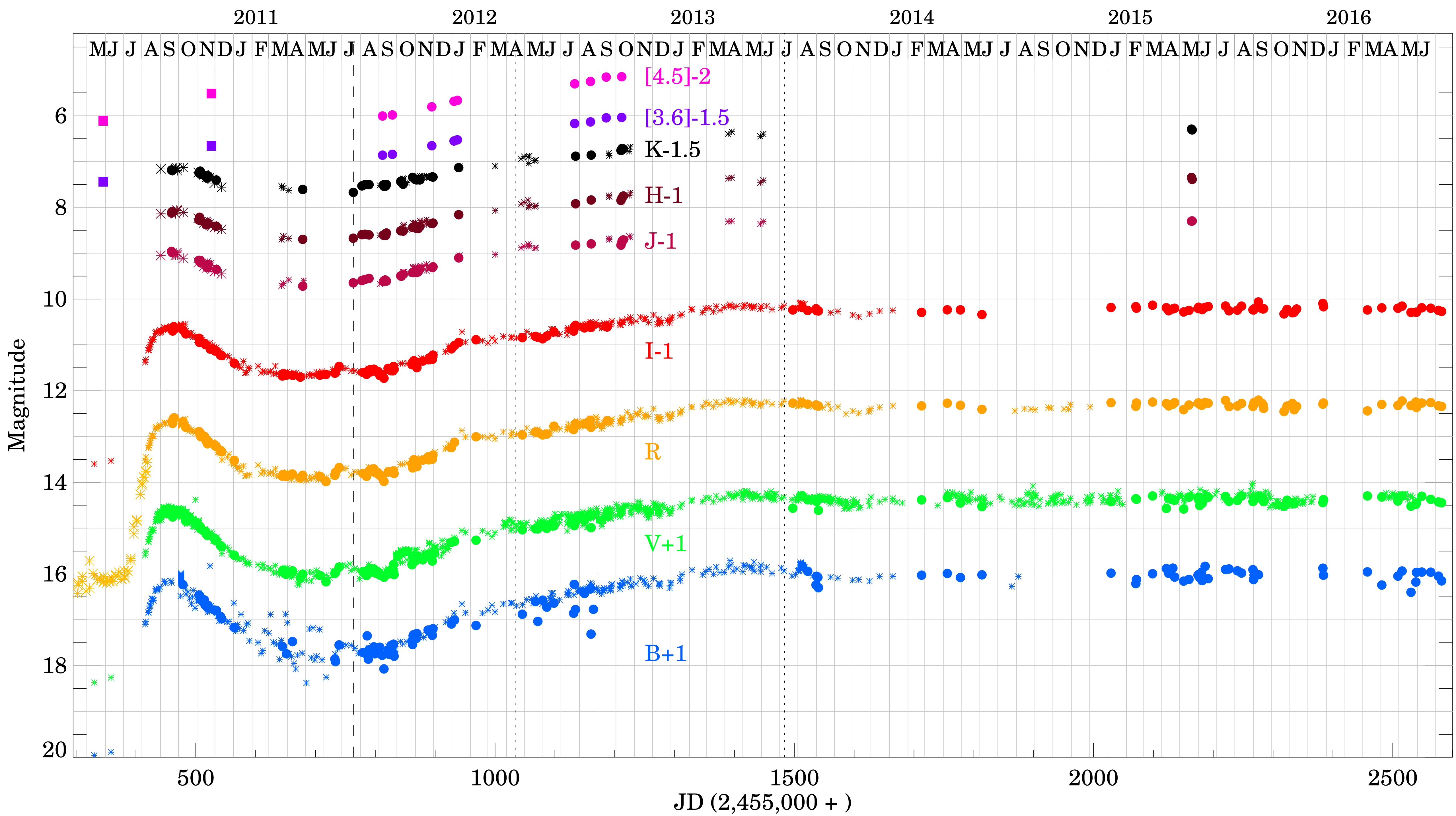


**Fig. 1.** Light curves of HBC 722. Filled dots are from Paper I and this work, plus signs are from Semkov et al. (2010), Semkov et al. (2014), Miller et al. (2011), Sung et al. (2013), Antoniucci et al. (2013), and from the AAVSO database[1]. Mid-IR data points are either from WISE (filled squares) or from *Spitzer* (filled dots). For clarity, the *B*, *V*, *I*, *J*, *H*, $K_S$, [3.6] and [4.5] light curves are shifted along the *y*-axis. The vertical dashed line marks the epoch when our near-IR LIRIS spectum was taken, while the vertical dotted lines indicate the time of our optical GTC/OSIRIS spectra.

The Astronomical Journal, 151:117 (8pp), 2016 May
doi:10.3847/0004-6256/151/5/117


# LARGE SIZE AND SLOW ROTATION OF THE TRANS-NEPTUNIAN OBJECT (225088) 2007 $OR_{10}$ DISCOVERED FROM *HERSCHEL* AND *K2* OBSERVATIONS

András Pál[1,2], Csaba Kiss[1], Thomas G. Müller[3], László Molnár[1], Róbert Szabó[1], Gyula M. Szabó[1,4,5], Krisztián Sárneczky[1,5], and László L. Kiss[1,5,6]

[1] Konkoly Observatory, Research Centre for Astronomy and Earth Sciences, Hungarian Academy of Sciences, H-1121 Budapest, Konkoly Thege Miklós út 15-17, Hungary; apal@szofi.net
[2] Eötvös Loránd Tudományegyetem, H-1117 Pázmány Péter sétány 1/A, Budapest, Hungary
[3] Max-Planck-Institut für extraterrestrische Physik, Postfach 1312, Giessenbachstr., D-85741 Garching, Germany
[4] ELTE Gothard Astrophysical Observatory, H-9704 Szombathely, Szent Imre herceg út 112, Hungary
[5] Gothard-Lendület Research Team, H-9704 Szombathely, Szent Imre herceg út 112, Hungary
[6] Sydney Institute for Astronomy, School of Physics A28, University of Sydney, NSW 2006, Australia
*Received 2015 September 24; accepted 2016 February 20; published 2016 April 19*

## ABSTRACT

We present the first comprehensive thermal and rotational analysis of the second most distant trans-Neptunian object (TNOs) (225088) 2007 $OR_{10}$. We combined optical light curves provided by the *Kepler Space Telescope–K2* extended mission and thermal infrared data provided by the *Herschel Space Observatory*. We found that (225088) 2007 $OR_{10}$ is likely to be larger and darker than derived by earlier studies: we obtained a diameter of $d = 1535^{+75}_{-225}$ km which places (225088) 2007 $OR_{10}$ in the biggest top three TNOs. The corresponding visual geometric albedo is $p_V = 0.089^{+0.031}_{-0.009}$. The light-curve analysis revealed a slow rotation rate of $P_{\rm rot} = 44.81 \pm 0.37$ hr, superseded by very few objects. The most likely light-curve solution is double-peaked with a slight asymmetry; however, we cannot safely rule out the possibility of having a rotation period of $P_{\rm rot} = 22.40 \pm 0.18$ hr, which corresponds to a single-peaked solution. Due to the size and slow rotation, the shape of the object should be a MacLaurin ellipsoid, so the light variation should be caused by surface inhomogeneities. Its newly derived larger diameter also implies larger surface gravity and a more likely retention of volatiles—$CH_4$, CO, and $N_2$—on the surface.

*Key words:* Kuiper belt objects: individual ((225088) $OR_{10}$) – methods: observational – minor planets, asteroids: general – radiation mechanisms: thermal – techniques: photometric

*Supporting material:* machine-readable table

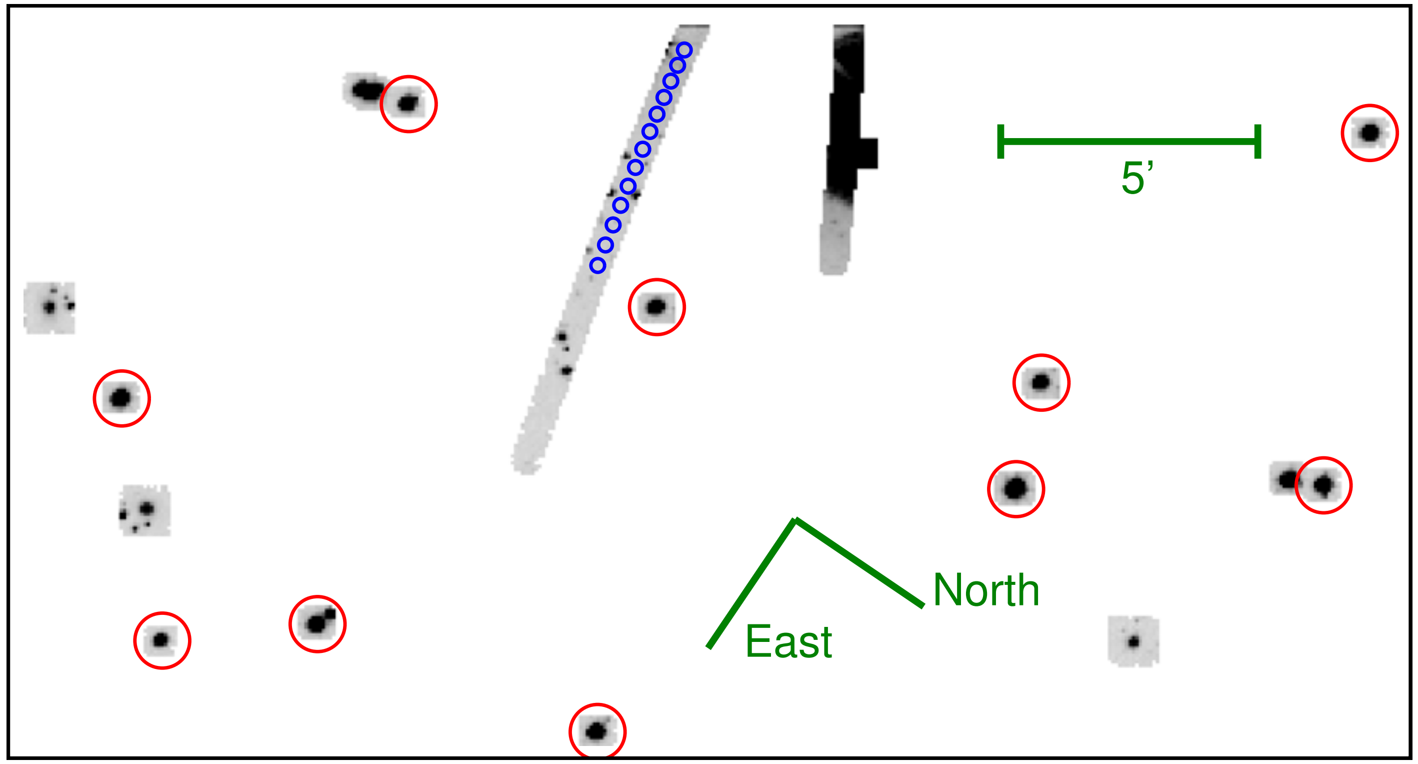


**Figure 1.** Total analyzed field of view of the *Kepler*, showing both the stamps related to (225088) 2007 $OR_{10}$ as well as the nearby image stamps used for astrometry. The stars used by the determination for both the differential and absolute astrometric solutions are indicated by red circles. The field has a pixel dimension of 410 × 220, equivalent to 27′ × 15′. Note that the pixels are shown in the reference frame of the detector and therefore the image itself is flipped. Note also that the edge of channel 2 of module #18 is at the top of the image.

The Astronomical Journal, 151:117 (8pp), 2016 May Pál et al.

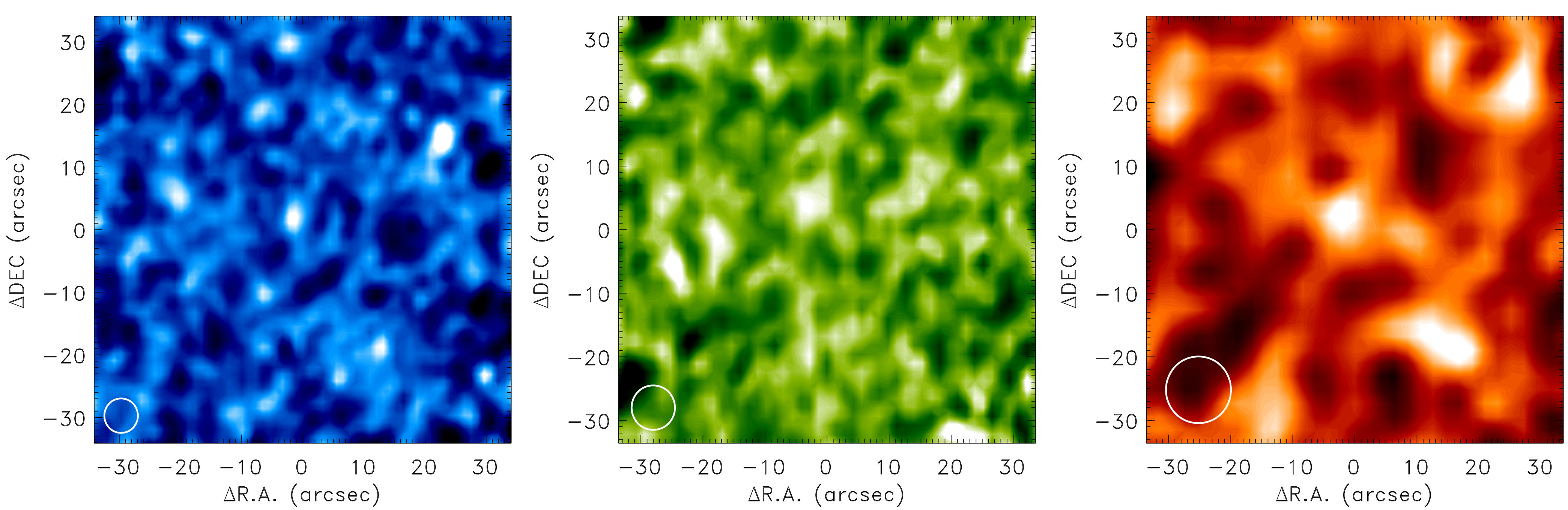


**Figure 2.** Image stamps of (225088) 2007 $OR_{10}$ as seen by the PACS detector of *Herschel*. The stamps show the vicinity of the object and cover a 70″ × 70″ area on the sky. From left to right, the stamps show the object in 70 $\mu$m (blue), 100 $\mu$m (green), and 160 $\mu$m (red) channels. The small white circles in the lower-left corner show the beam size (which is the largest in the red channel due to the diffraction-limited resolution of the instrument. Note that the object itself is slightly offset by ≈2″ from the field center due to the pointing drifts and astrometric uncertainties with respect to the nominal coordinates.

A&A 595, A2 (2016)
DOI: 10.1051/0004-6361/201629512


*Gaia Data Release 1*

Astronomy & Astrophysics
Special issue

# *Gaia* Data Release 1

## Summary of the astrometric, photometric, and survey properties

Gaia Collaboration, A. G. A. Brown[1,⋆], A. Vallenari[2], T. Prusti[3], J. H.J. de Bruijne[3], F. Mignard[4], R. Drimmel[5], C. Babusiaux[6], C. A.L. Bailer-Jones[7], U. Bastian[8], M. Biermann[8], D. W. Evans[9], L. Eyer[10], F. Jansen[11], C. Jordi[12], D. Katz[6], S. A. Klioner[13], U. Lammers[14], L. Lindegren[15], X. Luri[12], W. O'Mullane[14], C. Panem[16], D. Pourbaix[17,18], S. Randich[19], P. Sartoretti[6], H. I. Siddiqui[20], C. Soubiran[21], V. Valette[16], F. van Leeuwen[9], N. A. Walton[9], C. Aerts[22,23], F. Arenou[6], M. Cropper[24], E. Høg[25], M. G. Lattanzi[5], E. K. Grebel[8], A. D. Holland[26], C. Huc[16], X. Passot[16], M. Perryman[3], L. Bramante[27], C. Cacciari[28], J. Castañeda[12], L. Chaoul[16], N. Cheek[29], F. De Angeli[9], C. Fabricius[12], R. Guerra[14], J. Hernández[14], A. Jean-Antoine-Piccolo[16], E. Masana[12], R. Messineo[27], N. Mowlavi[10], K. Nienartowicz[30], D. Ordóñez-Blanco[30], P. Panuzzo[6], J. Portell[12], P. J. Richards[31], M. Riello[9], G. M. Seabroke[24], P. Tanga[4], F. Thévenin[4], J. Torra[12], S. G. Els[32,8], G. Gracia-Abril[32,12], G. Comoretto[20], M. Garcia-Reinaldos[14], T. Lock[14], E. Mercier[32,8], M. Altmann[8,33], R. Andrae[7], T. L. Astraatmadja[7], I. Bellas-Velidis[34], K. Benson[24], J. Berthier[35], R. Blomme[36], G. Busso[9], B. Carry[4,35], A. Cellino[5], G. Clementini[28], S. Cowell[9], O. Creevey[4,37], J. Cuypers[36], M. Davidson[38], J. De Ridder[22], A. de Torres[39], L. Delchambre[40], A. Dell'Oro[19], C. Ducourant[21], Y. Frémat[36], M. García-Torres[41], E. Gosset[40,18], J.-L. Halbwachs[42], N. C. Hambly[38], D. L. Harrison[9,43], M. Hauser[8], D. Hestroffer[35], S. T. Hodgkin[9], H. E. Huckle[24], A. Hutton[44], G. Jasniewicz[45], S. Jordan[8], M. Kontizas[46], A. J. Korn[47], A. C. Lanzafame[48,49], M. Manteiga[50], A. Moitinho[51], K. Muinonen[52,53], J. Osinde[54], E. Pancino[19,55], T. Pauwels[36], J.-M. Petit[56], A. Recio-Blanco[4], A. C. Robin[56], L. M. Sarro[57], C. Siopis[17], M. Smith[24], K. W. Smith[7], A. Sozzetti[5], W. Thuillot[35], W. van Reeven[44], Y. Viala[6], U. Abbas[5], A. Abreu Aramburu[58], S. Accart[59], J. J. Aguado[57], P. M. Allan[31], W. Allasia[60], G. Altavilla[28], M. A. Álvarez[50], J. Alves[61], R. I. Anderson[62,10], A. H. Andrei[63,64,33], E. Anglada Varela[54,29], E. Antiche[12], T. Antoja[3], S. Antón[65,66], B. Arcay[50], N. Bach[44], S. G. Baker[24], L. Balaguer-Núñez[12], C. Barache[33], C. Barata[51], A. Barbier[59], F. Barblan[10], D. Barrado y Navascués[67], M. Barros[51], M. A. Barstow[68], U. Becciani[49], M. Bellazzini[28], A. Bello García[69], V. Belokurov[9], P. Bendjoya[4], A. Berihuete[70], L. Bianchi[60], O. Bienaymé[42], F. Billebaud[21], N. Blagorodnova[9], S. Blanco-Cuaresma[10,21], T. Boch[42], A. Bombrun[39], R. Borrachero[12], S. Bouquillon[33], G. Bourda[21], H. Bouy[67], A. Bragaglia[28], M. A. Breddels[71], N. Brouillet[21], T. Brüsemeister[8], B. Bucciarelli[5], P. Burgess[9], R. Burgon[26], A. Burlacu[16], D. Busonero[5], R. Buzzi[5], E. Caffau[6], J. Cambras[72], H. Campbell[9], R. Cancelliere[73], T. Cantat-Gaudin[2], T. Carlucci[33], J. M. Carrasco[12], M. Castellani[74], P. Charlot[21], J. Charnas[30], A. Chiavassa[4], M. Clotet[12], G. Cocozza[28], R. S. Collins[38], G. Costigan[1], F. Crifo[6], N. J.G. Cross[38], M. Crosta[5], C. Crowley[39], C. Dafonte[50], Y. Damerdji[40,75], A. Dapergolas[34], P. David[35], M. David[76], P. De Cat[36], F. de Felice[77], P. de Laverny[4], F. De Luise[78], R. De March[27], D. de Martino[79], R. de Souza[80], J. Debosscher[22], E. del Pozo[44], M. Delbo[4], A. Delgado[9], H. E. Delgado[57], P. Di Matteo[6], S. Diakite[56], E. Distefano[49], C. Dolding[24], S. Dos Anjos[80], P. Drazinos[46], J. Duran[54], Y. Dzigan[81,82], B. Edvardsson[47], H. Enke[83], N. W. Evans[9], G. Eynard Bontemps[59], C. Fabre[84], M. Fabrizio[55,78], S. Faigler[85], A. J. Falcão[86], M. Farràs Casas[12], L. Federici[28], G. Fedorets[52], J. Fernández-Hernández[29], P. Fernique[42], A. Fienga[87], F. Figueras[12], F. Filippi[27], K. Findeisen[6], A. Fonti[27], M. Fouesneau[7], E. Fraile[88], M. Fraser[9], J. Fuchs[89], M. Gai[5], S. Galleti[28], L. Galluccio[4], D. Garabato[50], F. García-Sedano[57], A. Garofalo[28], N. Garralda[12], P. Gavras[6,34,46], J. Gerssen[83], R. Geyer[13], G. Gilmore[9], S. Girona[90], G. Giuffrida[55], M. Gomes[51], A. González-Marcos[91], J. González-Núñez[29,92], J. J. González-Vidal[12], M. Granvik[52], A. Guerrier[59], P. Guillout[42], J. Guiraud[16], A. Gúrpide[12], R. Gutiérrez-Sánchez[20], L. P. Guy[30], R. Haigron[6], D. Hatzidimitriou[46], M. Haywood[6], U. Heiter[47], A. Helmi[71], D. Hobbs[15], W. Hofmann[8], B. Holl[10], G. Holland[9], J. A.S. Hunt[24], A. Hypki[1], V. Icardi[27], M. Irwin[9], G. Jevardat de Fombelle[30], P. Jofré[9,21], P. G. Jonker[93,23], A. Jorissen[17], F. Julbe[12], A. Karampelas[46,34], A. Kochoska[94], R. Kohley[14], K. Kolenberg[95,22,96], E. Kontizas[34], S. E. Koposov[9], G. Kordopatis[83,4], P. Koubsky[89], A. Krone-Martins[51], M. Kudryashova[35], I. Kull[85], R. K. Bachchan[15], F. Lacoste-Seris[59], A. F. Lanza[49], J.-B. Lavigne[59], C. Le Poncin-Lafitte[33], Y. Lebreton[6,97], T. Lebzelter[61], S. Leccia[79], N. Leclerc[6], I. Lecoeur-Taibi[30], V. Lemaitre[59], H. Lenhardt[8], F. Leroux[59], S. Liao[5,98], E. Licata[60], H. E.P. Lindstrøm[25,99], T. A. Lister[100], E. Livanou[46], A. Lobel[36], W. Löffler[8], M. López[67], D. Lorenz[61], I. MacDonald[38], T. Magalhães Fernandes[86], S. Managau[59], R. G. Mann[38], G. Mantelet[8], O. Marchal[6], J. M. Marchant[101], M. Marconi[79], S. Marinoni[74,55], P. M. Marrese[74,55], G. Marschalkó[102,103], D. J. Marshall[104], J. M. Martín-Fleitas[44], M. Martino[27], N. Mary[59], G. Matijevič[83], T. Mazeh[85], P. J. McMillan[15], S. Messina[49],

D. Michalik[15], N. R. Millar[9], B. M. H. Miranda[51], D. Molina[12], R. Molinaro[79], M. Molinaro[105], L. Molnár[102], M. Moniez[106], P. Montegriffo[28], R. Mor[12], A. Mora[44], R. Morbidelli[5], T. Morel[40], S. Morgenthaler[107], D. Morris[38], A. F. Mulone[27], T. Muraveva[28], I. Musella[79], J. Narbonne[59], G. Nelemans[23,22], L. Nicastro[108], L. Noval[59], C. Ordénovic[4], J. Ordieres-Meré[109], P. Osborne[9], C. Pagani[68], I. Pagano[49], F. Pailler[16], H. Palacin[59], L. Palaversa[10], P. Parsons[20], M. Pecoraro[60], R. Pedrosa[110], H. Pentikäinen[52], B. Pichon[4], A. M. Piersimoni[78], F.-X. Pineau[42], E. Plachy[102], G. Plum[6], E. Poujoulet[111], A. Prša[112], L. Pulone[74], S. Ragaini[28], S. Rago[5], N. Rambaux[35], M. Ramos-Lerate[113], P. Ranalli[15], G. Rauw[40], A. Read[68], S. Regibo[22], C. Reylé[56], R. A. Ribeiro[86], L. Rimoldini[30], V. Ripepi[79], A. Riva[5], G. Rixon[9], M. Roelens[10], M. Romero-Gómez[12], N. Rowell[38], F. Royer[6], L. Ruiz-Dern[6], G. Sadowski[17], T. Sagristà Sellés[8], J. Sahlmann[14], J. Salgado[54], E. Salguero[54], M. Sarasso[5], H. Savietto[114], M. Schultheis[4], E. Sciacca[49], M. Segol[115], J. C. Segovia[29], D. Segransan[10], I.-C. Shih[6], R. Smareglia[105], R. L. Smart[5], E. Solano[67,116], F. Solitro[27], R. Sordo[2], S. Soria Nieto[12], J. Souchay[33], A. Spagna[5], F. Spoto[4], U. Stampa[8], I. A. Steele[101], H. Steidelmüller[13], C. A. Stephenson[20], H. Stoev[117], F. F. Suess[9], M. Süveges[30], J. Surdej[40], L. Szabados[102], E. Szegedi-Elek[102], D. Tapiador[118,119], F. Taris[33], G. Tauran[59], M. B. Taylor[120], R. Teixeira[80], D. Terrett[51], B. Tingley[121], S. C. Trager[71], C. Turon[6], A. Ulla[122], E. Utrilla[44], G. Valentini[78], A. van Elteren[1], E. Van Hemelryck[36], M. van Leeuwen[9], M. Varadi[10,102], A. Vecchiato[5], J. Veljanoski[71], T. Via[72], D. Vicente[90], S. Vogt[123], H. Voss[12], V. Votruba[89], S. Voutsinas[38], G. Walmsley[16], M. Weiler[12], K. Weingrill[83], T. Wevers[23], Ł. Wyrzykowski[9,124], A. Yoldas[9], M. Žerjal[94], S. Zucker[81], C. Zurbach[45], T. Zwitter[94], A. Alecu[9], M. Allen[3], C. Allende Prieto[24,125,126], A. Amorim[51], G. Anglada-Escudé[12], V. Arsenijevic[51], S. Azaz[3], P. Balm[20], M. Beck[30], H.-H. Bernstein[†,8], L. Bigot[4], A. Bijaoui[4], C. Blasco[127], M. Bonfigli[78], G. Bono[74], S. Boudreault[24,128], A. Bressan[129], S. Brown[9], P.-M. Brunet[16], P. Bunclark[†,9], R. Buonanno[74], A. G. Butkevich[13], C. Carret[110], C. Carrion[57], L. Chemin[21,130], F. Chéreau[6], L. Corcione[5], E. Darmigny[16], K. S. de Boer[131], P. de Teodoro[29], P. T. de Zeeuw[1,132], C. Delle Luche[6,59], C. D. Domingues[133], P. Dubath[30], F. Fodor[16], B. Frézouls[16], A. Fries[12], D. Fustes[50], D. Fyfe[68], E. Gallardo[12], J. Gallegos[29], D. Gardiol[5], M. Gebran[12,134], A. Gomboc[94,135], A. Gómez[6], E. Grux[56], A. Gueguen[6,136], A. Heyrovsky[38], J. Hoar[14], G. Iannicola[74], Y. Isasi Parache[12], A.-M. Janotto[16], E. Joliet[39,137], A. Jonckheere[36], R. Keil[138,139], D.-W. Kim[7], P. Klagyivik[102], J. Klar[83], J. Knude[25], O. Kochukhov[47], I. Kolka[140], J. Kos[94,141], A. Kutka[89,142], V. Lainey[35], D. LeBouquin[59], C. Liu[7,143], D. Loreggia[5], V. V. Makarov[144], M. G. Marseille[59], C. Martayan[36,145], O. Martinez-Rubi[12], B. Massart[4,59,146], F. Meynadier[6,33], S. Mignot[6], U. Munari[2], A.-T. Nguyen[16], T. Nordlander[47], P. Ocvirk[83,42], K. S. O'Flaherty[147], A. Olias Sanz[148], P. Ortiz[68], J. Osorio[65], D. Oszkiewicz[52,149], A. Ouzounis[38], M. Palmer[12], P. Park[10], E. Pasquato[17], C. Peltzer[9], J. Peralta[12], F. Péturaud[6], T. Pieniluoma[52], E. Pigozzi[27], J. Poels[†,40], G. Prat[150], T. Prod'homme[1,151], F. Raison[152,136], J. M. Rebordao[133], D. Risquez[1], B. Rocca-Volmerange[153], S. Rosen[24,68], M. I. Ruiz-Fuertes[30], F. Russo[5], S. Sembay[68], I. Serraller Vizcaino[154], A. Short[3], A. Siebert[42,83], H. Silva[86], D. Sinachopoulos[34], E. Slezak[4], M. Soffel[13], D. Sosnowska[10], V. Straižys[155], M. ter Linden[39,156], D. Terrell[157], S. Theil[158], C. Tiede[7,159], L. Troisi[55,160], P. Tsalmantza[7], D. Tur[72], M. Vaccari[161,162], F. Vachier[35], P. Valles[12], W. Van Hamme[163], L. Veltz[83,37], J. Virtanen[52,53], J.-M. Wallut[16], R. Wichmann[164], M. I. Wilkinson[9,68], H. Ziaeepour[56], and S. Zschocke[13]

*(Affiliations can be found after the references)*

Received 10 August 2016 / Accepted 31 August 2016

The Astrophysical Journal Supplement Series, 224:41 (23pp), 2016 June doi:10.3847/0067-0049/224/2/41


# UNEXPECTED SERIES OF REGULAR FREQUENCY SPACING OF $\delta$ SCUTI STARS IN THE NON-ASYMPTOTIC REGIME. II. SAMPLE–ECHELLE DIAGRAMS AND ROTATION

M. Paparó[1], J. M. Benkő[1], M. Hareter[1], and J. A. Guzik[2]
[1] Konkoly Observatory, MTA CSFK, Konkoly Thege Miklós út 15-17., H-1121 Budapest, Hungary; paparo@konkoly.hu
[2] Los Alamos National Laboratory, Los Alamos, NM 87545, USA
*Received 2015 October 15; accepted 2016 March 24; published 2016 June 17*

## ABSTRACT

A sequence search method was developed for searching for regular frequency spacing in $\delta$ Scuti stars by visual inspection (VI) and algorithmic search. The sample contains 90 $\delta$ Scuti stars observed by *CoRoT*. An example is given to represent the VI. The algorithm (SSA) is described in detail. The data treatment of the *CoRoT* light curves, the criteria for frequency filtering, and the spacings derived by two methods (i.e., three approaches: VI, SSA, and FT) are given for each target. Echelle diagrams are presented for 77 targets for which at least one sequence of regular spacing was identified. Comparing the spacing and the shifts between pairs of echelle ridges revealed that at least one pair of echelle ridges is shifted to midway between the spacing for 22 stars. The estimated rotational frequencies compared to the shifts revealed rotationally split doublets, triplets, and multiplets not only for single frequencies, but for the complete echelle ridges in 31 $\delta$ Scuti stars. Using several possible assumptions for the origin of the spacings, we derived the large separation ($\Delta\nu$) that are distributed along the mean density versus large separations relation derived from stellar models.

*Key words:* space vehicles – stars: oscillations (including pulsations) – stars: variables: delta Scuti – techniques: photometric

*Supporting material:* machine-readable table

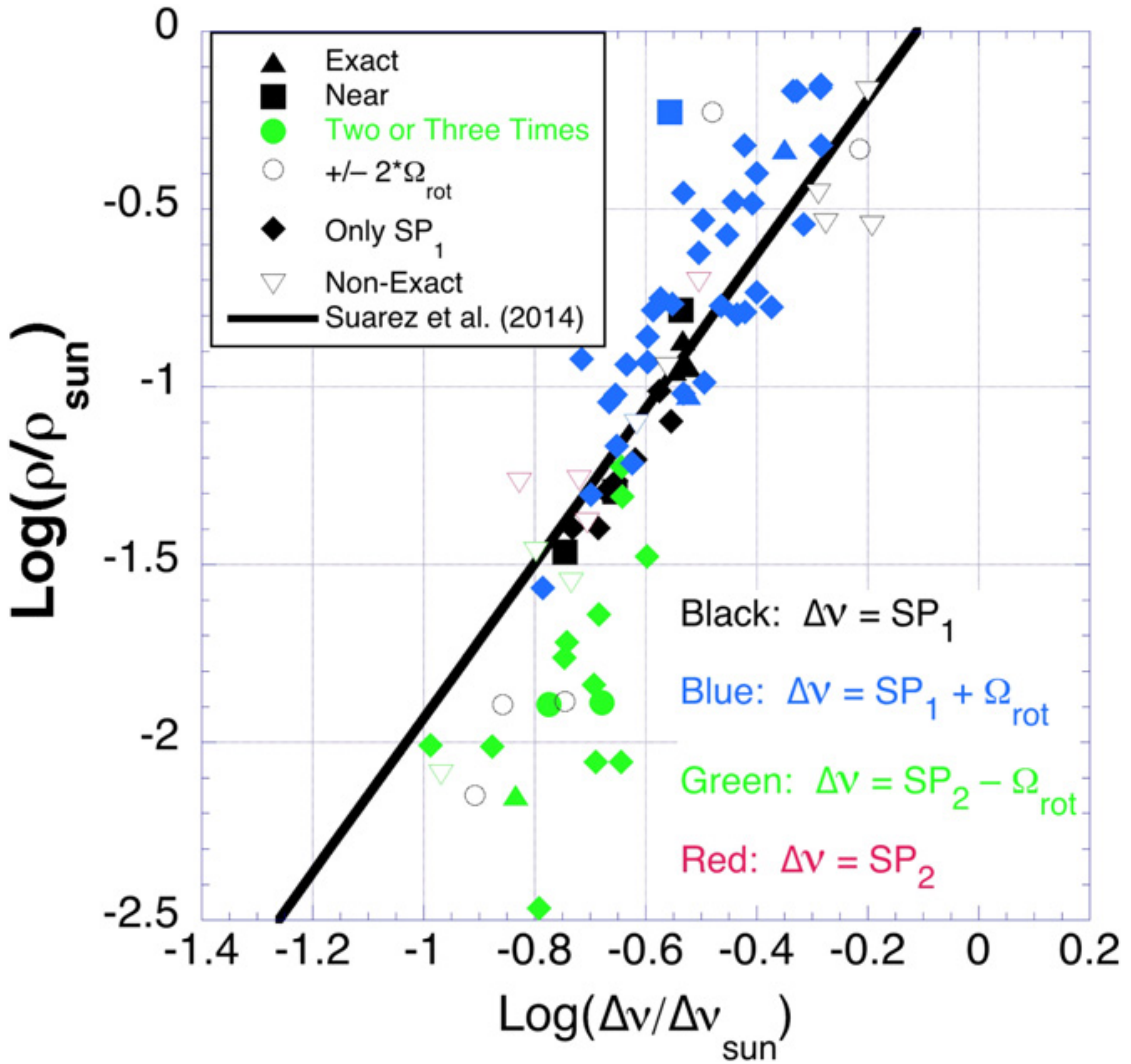


**Figure 16.** Location of the whole sample on the log mean density vs. log large separation diagram, along with the relation based on stellar models from Suárez et al. (2014). The new symbols represent the stars for which there is no agreement between the rotational frequency and the difference of the spacings (inverted triangle) or the stars with only one spacing (diamonds). The color code is the same as in the previous figure, with the addition of the red color corresponding to $\Delta\nu = \mathrm{SP}_2$.